

# Internal Boundary Control of Lane-free Automated Vehicle Traffic using a Linear Quadratic Integral Regulator\*

Milad Malekzadeh, Ioannis Papamichail, Markos Papageorgiou, *Life Fellow, IEEE*

**Abstract**— Lane-free traffic has been recently proposed for connected automated vehicles (CAV). As incremental changes of the road width in lane-free traffic lead to corresponding incremental changes of the traffic flow capacity, the concept of internal boundary control can be used to optimize infrastructure utilization. Internal boundary control leads to flexible sharing of the total road width and capacity among the two traffic directions (of a highway or an arterial) in real-time, in response to the prevailing traffic conditions. A feedback-based Linear-Quadratic regulator with Integral action (LQI regulator) is appropriately developed in this paper to efficiently address this problem. Simulation investigations, involving a realistic highway stretch, demonstrate that the proposed simple LQI regulator is robust and very efficient.

## I. INTRODUCTION

Recurrent traffic congestion is an increasingly serious problem for most big cities worldwide, causing substantial delays, increased fuel consumption, excessive environmental pollution and reduced traffic safety. Conventional traffic management measures are valuable [1], [2] and, in some cases, able to delay or even avoid the onset of congestion. However, they are not always sufficient to tackle heavily congested traffic conditions. Gradually emerging and future ground-breaking vehicle automation and communication systems should be exploited to develop innovative solutions that can be applied within a smart road infrastructure. During the last decade, there has been an enormous effort by the industry and by many research institutions to develop and deploy a variety of vehicle automation and communication systems that are revolutionizing the vehicle capabilities [3].

Recently, the TrafficFluid concept was launched [4]. This is a novel paradigm for vehicular traffic that is appropriate for high penetration rates of vehicles equipped with high levels of vehicle automation and communication systems. The TrafficFluid concept suggests: (1) lane-free traffic, whereby vehicles are not bound to fixed traffic lanes, as in conventional traffic; (2) vehicle nudging, whereby vehicles may exert a "nudging" effect on, i.e. influence the movement of vehicles in front of them. In this context, the internal boundary control concept, introduced in [5], exploits the lane-free principle of TrafficFluid. In lane-free traffic, the road capacity may exhibit incremental (increasing or decreasing) changes in response to corresponding incremental (widening or narrowing) changes of the road width. This is in contrast to lane-based traffic, where capacity

changes may only occur if the road width is changed by one or more lanes.

Consider a road with two opposite traffic directions serving connected automated vehicles (CAVs). The total available cross-road capacity (for both directions) may be shared among the two directions in a flexible way, according to the prevailing demand per direction. Flexible capacity sharing may be achieved by virtually moving the internal boundary that separates the two traffic directions and communicating this decision to CAVs, so that they respect the road boundary. This way, the total capacity share assigned per direction can be changed in space and time according to an appropriate real-time control strategy, as illustrated in Fig. 1, in order to maximize the traffic efficiency of the overall system.

The idea of sharing the total cross-road capacity among the two traffic directions is not new as it has been occasionally employed for conventional lane-based traffic, typically with manual interventions [6]. The measure is known as tidal flow (or reversible lanes) control and its main principle is to adapt the total available supply to the demand per direction. Its most basic form is the steady allocation of one or more lanes of one direction to the other direction for a period of time so as to address abnormal traffic supply or demand. More advanced reversible lane control systems may operate in real time, e.g. to balance delays on both sides of a known bottleneck (e.g. bridge, tunnel) by assigning a lane to one of the two directions in alternation in response to the prevailing traffic conditions. In order to deal with this problem, optimal control or feedback control algorithms of various types were proposed [7], [8].

Reversible lanes have also been considered in connection with lane-based CAV driving. The system optimal dynamic traffic assignment models formulated in [9], [10], using the Cell Transmission Model (CTM) [11] are utilized in [12]. Lanes are introduced as integer variables, and the problem is formulated as a mixed integer linear programming (MILP) problem that has, however, high (exponential) complexity due to the many integers variables involved. The same model is used in [13] for a single link and stochastic demand is utilized as a Markov decision process while the MILP problem is solved using a heuristic.

The use of tidal flow control systems in lane-based traffic

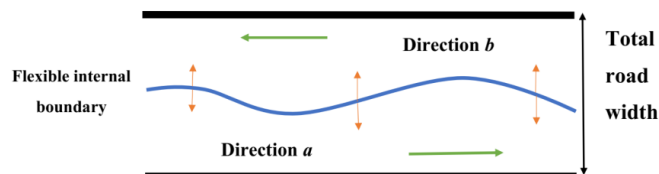


Fig. 1. Space-time flexible internal road boundary.

\*The research leading to these results has received funding from the European Research Council under the European Union's Horizon 2020 Programme / ERC Grant Agreement no. 833915, project TrafficFluid, see: <https://www.trafficfluid.tuc.gr>.

All authors are with the Dynamic Systems and Simulation Laboratory, Technical University of Crete, Chania, Crete, 73100, Greece (e-mails: mmalek@dssl.tuc.gr, ipapa@dssl.tuc.gr, markos@dssl.tuc.gr).

is not widespread for a number of reasons, including the harsh resolution of infrastructure sharing (only by lane quanta) among the two traffic directions; the serious counter-problems due to frequent merging or diverging traffic at lane-drop or lane-gain areas; and the safety-induced time-delays after each lane switch. These serious difficulties entail very limited capacity sharing flexibility in space and time and hinder reversible lane control from being a major traffic management measure. Even in the future CAV traffic, some of the mentioned difficulties would persist in lane-based conditions, notably the low capacity sharing resolution and the merging nuisance. In contrast, in a lane-free CAV traffic environment, the mentioned difficulties are largely mitigated. More specifically, the resolution of road-width sharing among the two directions can be high; the smooth CAV driving on a lane-free road surface allows for the internal boundary to be a smooth space-function, as illustrated in Fig. 1; while assuming moderate changes of the internal boundary over time and space, the aforementioned safety-induced time-delay may be very small.

Thanks to these characteristics, real-time internal boundary control for lane-free CAV traffic may be broadly applicable to the high number of arterial or highway infrastructures that feature unbalanced demands during the day in the two traffic directions, so as to strongly mitigate or even utterly avoid congestion. Even for infrastructures experiencing strong demand in both directions quasi-simultaneously, real-time internal boundary control may intensify the road utilization and lead to sensible improvements.

The internal boundary control problem is analyzed in [5], where its high improvement potential is demonstrated by formulating and solving an open-loop optimal control problem, in the form of a convex Quadratic Programming (QP) problem. That approach may be used within an MPC (Model Predictive Control) frame for real-time application, but simpler real-time approaches with similar efficiency are preferable. This paper develops and investigates the application of a Linear-Quadratic regulator with Integral action (LQI regulator) for the internal boundary control problem. The LQI regulator leads to a simpler real-time algorithm and does not require prediction of external demands as the QP-based approach. The well-known CTM is used, after linearization, for controller design; and, in its full nonlinear form, for simulation testing. The performance of the LQI regulator is compared to the no-control case. Section II presents some background issues and the appropriately adjusted CTM equations, while Section III presents the design of the LQI regulator. Simulation investigations are discussed in Section IV, while conclusions are given in Section V.

## II. BACKGROUND

Lane-free traffic is not expected to give rise to structural changes of existing macroscopic traffic flow models. As also supported by results in [4], [14]-[16], notions and concepts like the conservation equation, the Fundamental Diagram (FD), as well as moving traffic waves will continue to characterize macroscopic traffic flow modelling in the case of lane-free CAV traffic. Additionally, specific physical traffic parameters, such as free speed, critical density, flow capacity,

jam density, are also relevant for lane-free traffic, but may of course take different values than in lane-based traffic.

Let us call the two opposite traffic directions, presented in Fig. 1, directions  $a$  and  $b$ , respectively. We will assume that, at specific road sections, each direction is assigned a respective road width  $w^a = \varepsilon \cdot w$  and  $w^b = (1 - \varepsilon) \cdot w$ , where  $0 \leq \varepsilon \leq 1$  is the sharing factor, to be specified in real time as a control input by the internal boundary controller, and  $w$  is the total road width (both directions).

Let  $Q(\rho)$ , where  $\rho$  is the traffic density in veh/km, be the FD of a road section, which would apply if the whole road width would be assigned to only one of the two opposite traffic directions (i.e. for  $\varepsilon$  equal 0 or 1), with total critical density  $\rho_{cr}$ , total capacity  $q_{cap}$  (in veh/h) and total jam density  $\rho_{max}$ . Let us now consider the case of partial road sharing, i.e.  $\varepsilon_{min} \leq \varepsilon \leq \varepsilon_{max}$ , where  $\varepsilon_{min}, \varepsilon_{max} \in (0, 1)$  are appropriate bounds aiming to suppress utter closure of either direction. The FDs for the two directions are functions of  $\varepsilon$  given by

$$\begin{aligned} Q^a(\rho^a, \varepsilon) &= \varepsilon \cdot Q(\rho^a / \varepsilon) \\ Q^b(\rho^b, \varepsilon) &= (1 - \varepsilon) \cdot Q(\rho^b / (1 - \varepsilon)) \end{aligned} \quad (1)$$

where  $\rho^a$  and  $\rho^b$  (in veh/km) are the respective densities of the two directions [5].

For controller design, a dynamic traffic flow model must be used. A simple but realistic option is CTM, a first-order dynamic traffic flow model with a triangular FD, which attains a space-time discretized form by application of the Godunov numerical scheme. CTM is presented in this section, along with appropriate adjustments introduced to incorporate the effect of the sharing factor  $\varepsilon$ .

Consider a highway stretch with two reverse traffic directions  $a$  (from left to right) and  $b$  (from right to left). The stretch is subdivided into  $n$  sections, with lengths  $L_i$ ,  $i = 1, 2, \dots, n$ . As explained above, the total road width, which is assumed constant over all sections for simplicity, can be flexibly shared among the two directions in real time. As the sharing may be different for every section, we have corresponding sharing factors  $\varepsilon_i$ ,  $i = 1, 2, \dots, n$ ; and (1) applies to each section. As a consequence, the total section capacity, as well as the critical density and jam density, are shared among traffic directions  $a$  and  $b$  according to

$$\begin{aligned} q_{i,cap}^a(\varepsilon_i) &= \varepsilon_i \cdot q_{cap}, \quad q_{i,cap}^b(\varepsilon_i) = (1 - \varepsilon_i) \cdot q_{cap} \\ \rho_{i,cr}^a(\varepsilon_i) &= \varepsilon_i \cdot \rho_{cr}, \quad \rho_{i,cr}^b(\varepsilon_i) = (1 - \varepsilon_i) \cdot \rho_{cr} \\ \rho_{i,max}^a(\varepsilon_i) &= \varepsilon_i \cdot \rho_{max}, \quad \rho_{i,max}^b(\varepsilon_i) = (1 - \varepsilon_i) \cdot \rho_{max} \end{aligned} \quad (2)$$

The above derivations rely on the assumption, partially verified in [4], that any incremental widening (narrowing) of the road width entails a corresponding incremental increase (decrease) of capacity. Indeed, the highway may hold vehicles of different dimensions and speeds. These vehicles spread, in a lane-free road structure, on the road surface according to their two-dimensional movement strategies, which lead to a variety of lateral vehicle positions, including vehicles driving on the road boundary (without ever exceeding it). Thus, every incremental widening of the road increases the average two-dimensional inter-vehicle spacing and offers possibilities for higher speed, and hence higher flow and capacity.

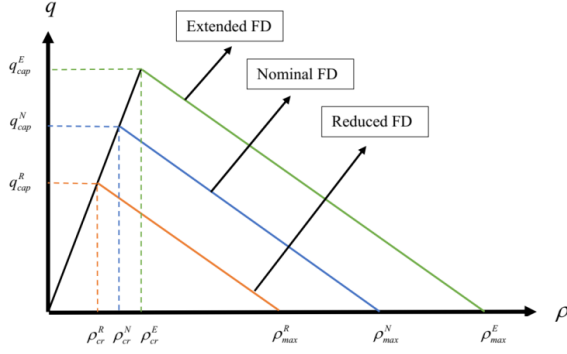


Fig. 2. The triangular fundamental diagram with flexible internal boundary.

The corresponding changes of the triangular FD that may occur at each section and traffic direction are illustrated in Fig. 2. More specifically, when the value of the sharing factor is 0.5, i.e., the flow capacities of the two directions are equal, their FDs are "nominal" (blue line with  $(\cdot)^N$  parameters); when the sharing factor is different than 0.5, we have two FDs: the extended one (green line with  $(\cdot)^E$  parameters) applies to the direction that is assigned more width and hence more flow capacity, and the reduced, complementary FD (orange line with  $(\cdot)^R$  parameters) applies to the other direction that is assigned less width and flow capacity. Based on (2), all FD parameters of a section change, whenever it is decided to change the corresponding sharing factor in real time.

For the internal boundary control problem, we would like to disallow the utter closure of either direction; hence, the assigned road width in either direction should never be smaller than the widest vehicles driving on the road. This requirement gives rise to stricter constraints for the sharing factors as follows

$$0 < \varepsilon_{i,\min} \leq \varepsilon_i \leq \varepsilon_{i,\max} < 1 \quad (3)$$

where  $\varepsilon_{i,\min} \cdot w$  and  $(1 - \varepsilon_{i,\max}) \cdot w$  are the minimum admissible widths to be assigned to directions  $a$  and  $b$ , respectively.

Another restriction to be applied to the sharing factors concerns the time-delay needed to evacuate traffic on the direction that receives a restricted width, compared with the previous control time-step. This time-delay is small in lane-free CAV traffic with moderate changes of the sharing factors applied to short sections. This time-delay is omitted here for simplicity and will be considered in a more comprehensive work.

Traffic flows from section 1 to section  $n$  in direction  $a$ ; and from section  $n$  to section 1 in direction  $b$  (see Fig. 3 as an example). We denote  $\rho_i^a$ ,  $i = 1, 2, \dots, n$ , the traffic density of section  $i$ , direction  $a$ ; and  $\rho_i^b$ ,  $i = 1, 2, \dots, n$ , the traffic density of section  $i$ , direction  $b$ . Similarly, we denote  $q_i^a$ ,  $i = 1, 2, \dots, n$ , and  $q_i^b$ ,  $i = 1, 2, \dots, n$ , the mainstream exit flows of section  $i$  for directions  $a$  and  $b$ , respectively. Thus,  $q_0^a$  is the feeding upstream mainstream inflow for direction  $a$ ; and  $q_{n+1}^b$  is the feeding upstream mainstream inflow for direction  $b$ . Every section may have an on-ramp or an off-ramp at its upstream boundary. The on-ramp flows (if any) at section  $i$  are denoted  $r_i^a$  for direction  $a$ , and  $r_i^b$  for direction  $b$ . The off-ramp flow (if any) of section  $i$ , direction  $a$ , is calculated based on known exit rates  $\beta_i^a$

multiplied with the upstream-section flow, i.e.  $\beta_i^a q_{i-1}^a$ ; and the off-ramp flow (if any) of section  $i$ , direction  $b$ , is calculated based on known exit rates  $\beta_i^b$  multiplied with the upstream-section flow, i.e.  $\beta_i^b q_{i+1}^b$ .

The conservation equation for the section  $i$  of direction  $a$  is:

$$\rho_i^a(k+1) = \rho_i^a(k) + \frac{T}{L_i} ((1 - \beta_i^a) q_{i-1}^a(k) - q_i^a(k) + r_i^a(k)) \quad (4)$$

where  $T$  is the model time-step, typically set equal to 5 – 10 s for section lengths of some 500 m in length, and  $k = 0, 1, \dots$  is the corresponding discrete time index of the model.

According to CTM, traffic flow is obtained as the minimum of demand and supply functions, except for the last section, where only the demand function is considered, assuming that the downstream traffic conditions are uncongested. Clearly, when writing the demand and supply functions  $Q_D$  and  $Q_S$ , respectively, for the case of the internal boundary control problem, we need to consider the impact of the respective sharing factors  $\varepsilon_i(k)$  on the FDs. Thus we have

$$q_i^a(k) = \min \left\{ Q_D(\rho_i^a(k), \varepsilon_i(k)), \frac{Q_S(\rho_{i+1}^a(k), \varepsilon_{i+1}(k))}{(1 - \beta_{i+1}^a)} - r_{i+1}^a(k) \right\},$$

$$i = 1, 2, \dots, n-1$$

$$q_n^a(k) = Q_D(\rho_n^a(k), \varepsilon_n(k)) \quad (5)$$

The demand and supply functions are given by the following respective equations

$$Q_D(\rho, \varepsilon) = \min \{ \varepsilon q_{cap}, v_f \rho \}$$

$$Q_S(\rho, \varepsilon) = \min \{ \varepsilon q_{cap}, w_s (\varepsilon \rho_{\max} - \rho) \} \quad (6)$$

where  $v_f$  is the free speed (which is assumed equal for all sections for simplicity) and  $w_s$  is the back-wave speed.

The equations for section  $i$  of direction  $b$  are analogous to those of direction  $a$ , with few necessary index modifications. Section numbers in direction  $b$  are descending, hence we have

$$\rho_i^b(k+1) = \rho_i^b(k) + \frac{T}{L_i} ((1 - \beta_i^b) q_{i+1}^b(k) - q_i^b(k) + r_i^b(k)) \quad (7)$$

and the flows are given by

$$q_i^b(k) = Q_D(\rho_i^b(k), (1 - \varepsilon_i(k)))$$

$$q_i^b(k) = \min \left\{ Q_D(\rho_i^b(k), (1 - \varepsilon_i(k))), \frac{Q_S(\rho_{i-1}^b(k), (1 - \varepsilon_{i-1}(k)))}{(1 - \beta_{i-1}^b)} - r_{i-1}^b(k) \right\}, i = 2, 3, \dots, n \quad (8)$$

### III. LQI REGULATOR DESIGN

#### A. Relative Densities

In conventional traffic management, traffic densities have a central role, as they reflect explicitly the state of traffic. However, in the novel internal boundary control setting the variables  $\rho_i^a$  and  $\rho_i^b$  of the traffic densities (in veh/km) in the two opposite directions of each section  $i$  are not directly indicating the traffic conditions (e.g. under-critical or congested) encountered. This is because the critical density for each direction is a function of the sharing factor and is

changing according to the applied control action. Therefore, we proceed with the definition of the *relative densities* (dimensionless) that are defined per section and per direction as the ordinary densities. The relative density of section  $i$  and direction  $a$  or  $b$  is obtained by dividing the corresponding traffic density with the corresponding critical density, which, on its turn, depends on the sharing factor prevailing during the last time-step. Considering (2), we get the following relations for section  $i$

$$\tilde{\rho}_i^a(k) = \frac{\rho_i^a(k)}{\varepsilon_i(k-1)\rho_{cr}}, \quad \tilde{\rho}_i^b(k) = \frac{\rho_i^b(k)}{(1-\varepsilon_i(k-1))\rho_{cr}} \quad (9)$$

### B. Linearized Model

In order to derive the LQI regulator, we need to include in our problem a discrete-time linearized system. To this end, we use as a basis the CTM equations delivered in the previous section. Replacing (9) in (4), i.e. in the conservation equation for direction  $a$ , and by dividing with  $\varepsilon_i(k-1)\rho_{cr}$  we get

$$\frac{\varepsilon_i(k)}{\varepsilon_i(k-1)} \tilde{\rho}_i^a(k+1) = \tilde{\rho}_i^a(k) + \frac{T}{L_i\rho_{cr}} \left( (1-\beta_i^a) \frac{q_{i-1}^a(k)}{\varepsilon_i(k-1)} - \frac{q_i^a(k)}{\varepsilon_i(k-1)} + \frac{r_i^a(k)}{\varepsilon_i(k-1)} \right) \quad (10)$$

It is now assumed that the values of the control inputs do not change significantly in consecutive sample times, i.e. that  $\varepsilon_i(k)/\varepsilon_i(k-1) \approx 1$ . Defining also the one-step retarded control input as a new state variable according to

$$\gamma_i(k+1) = \varepsilon_i(k), \quad i = 1, 2, \dots, n \quad (11)$$

we finally get the state equations that replace the conservation equations for section  $i$  of direction  $a$

$$\tilde{\rho}_i^a(k+1) = \tilde{\rho}_i^a(k) + \frac{T}{L_i\rho_{cr}} \left( (1-\beta_i^a) \frac{q_{i-1}^a(k)}{\gamma_i(k)} - \frac{q_i^a(k)}{\gamma_i(k)} + \frac{r_i^a(k)}{\gamma_i(k)} \right) \quad (12)$$

Similarly, replacing (9) in (7), i.e. in the conservation equation for direction  $b$ , and making the same assumption for the value of the control input in consecutive sample times, we get the state equations that replace the conservation equations for section  $i$  of direction  $b$

$$\tilde{\rho}_i^b(k+1) = \tilde{\rho}_i^b(k) + \frac{T}{L_i\rho_{cr}} \left( (1-\beta_i^b) \frac{q_{i+1}^b(k)}{1-\gamma_i(k)} - \frac{q_i^b(k)}{1-\gamma_i(k)} + \frac{r_i^b(k)}{1-\gamma_i(k)} \right) \quad (13)$$

According to CTM, traffic flow is obtained as the minimum of the demand and supply functions. Starting from CTM, we need to come up with an approximate linearized system to allow for the derivation of a feedback controller by use of the LQ regulator methodology. This is a procedure with a long history in traffic management and control, see e.g. [17]-[19]. In such works, the nominal linearization state (density) is taken to be uncongested and close to the critical density. Following this procedure in our case, we assume that traffic flow is nominally operating around capacity and is determined only by the demand function; which however is also obtained as the minimum of two terms according to (6), namely as the minimum of the flow capacity and the FD

flow-density relation. In conventional traffic control, the flow capacity is constant; hence a linear or linearized flow-density relation is taken from the FD to characterize the linear flow dynamics. In contrast, in the internal boundary control case, the capacity is directly proportional to the control input (sharing factor), as evidenced from (6), hence this term is deemed more significant in the linearized approximation of the system dynamics.

In conclusion, to proceed with the linearized approximation of system dynamics, flow is given as a convex combination of the two terms included in the min-operator of the demand function, i.e.  $q_i^a(k)$  is set equal to  $\sigma\varepsilon_i(k)q_{cap} + (1-\sigma)v_f\rho_i^a(k)$ ; and  $q_i^b(k)$  is set equal to  $\sigma(1-\varepsilon_i(k))q_{cap} + (1-\sigma)v_f\rho_i^b(k)$ , where  $0 \leq \sigma \leq 1$  is the convex combination parameter used. Taking into account (9) and (11),  $q_i^a(k)$  and  $q_i^b(k)$  are finally given by

$$q_i^a(k) = \sigma\varepsilon_i(k)q_{cap} + (1-\sigma)v_f\rho_i^a(k) \quad (14)$$

$$q_i^b(k) = \sigma(1-\varepsilon_i(k))q_{cap} + (1-\sigma)v_f\rho_i^b(k) \quad (15)$$

Considering this, the linearization of the system of dynamic equations (11)-(13) around a nominal point yields the linear state-space model

$$\mathbf{Ax}(k+1) = \mathbf{A}\mathbf{x}(k) + \mathbf{B}\mathbf{u}(k) \quad (16)$$

where  $\mathbf{Ax}(k) = [\Delta\tilde{\rho}^a(k)^T, \Delta\tilde{\rho}^b(k)^T, \Delta\gamma(k)^T]^T$  is the state vector and  $\mathbf{Au}(k) = \Delta\varepsilon(k)$  is the control vector, whereby  $\Delta\tilde{\rho}^a(k) = [\Delta\tilde{\rho}_1^a(k), \dots, \Delta\tilde{\rho}_n^a(k)]^T$ ,  $\Delta\tilde{\rho}^b(k) = [\Delta\tilde{\rho}_1^b(k), \dots, \Delta\tilde{\rho}_n^b(k)]^T$ ,  $\Delta\gamma(k) = [\Delta\gamma_1(k), \dots, \Delta\gamma_n(k)]^T$  and  $\Delta\varepsilon(k) = [\Delta\varepsilon_1(k), \dots, \Delta\varepsilon_n(k)]^T$ . Also,  $\Delta(\cdot)(k) = (\cdot)(k) - (\cdot)^N$ , the superscript  $N$  denotes the nominal point and it has been assumed that  $\Delta(\cdot)(k) = 0$  for all disturbances (upstream mainstream inflow, as well as the on-ramp flows of each direction).  $\mathbf{A} \in \mathbb{R}^{3n \times 3n}$  and  $\mathbf{B} \in \mathbb{R}^{3n \times n}$  are the state and input matrices, respectively.

If the control time-step is defined as a multiple of the model time-step, i.e.  $T_c = MT$ , where  $M$  is an integer, then the discrete control time index is  $k_c = \lfloor kT/T_c \rfloor$ . Then, the linear state-space equation may be changed as follows, in order to be based on the control time-step  $T_c$ ,

$$\mathbf{Ax}(k_c+1) = \mathbf{A}^M \mathbf{Ax}(k_c) + \hat{\mathbf{B}}\mathbf{u}(k_c) \quad (17)$$

where  $\hat{\mathbf{B}} = (\mathbf{A}^{M-1} + \mathbf{A}^{M-2} + \dots + \mathbf{I})\mathbf{B}$ .

### C. Integration States and Quadratic Cost Function

To enable the inclusion of integral terms in the regulator, we consider the state equation (17) augmented by use of the integrators

$$\mathbf{y}(k_c+1) = \mathbf{y}(k_c) + \underbrace{[\mathbf{I}_n, -\mathbf{I}_n, \mathbf{0}_{n \times n}]}_{\mathbf{H}} \mathbf{Ax}(k_c) \quad (18)$$

With this choice of integration state variables, we aim to integrate and achieve a steady-state error equal to zero for the differences between the relative densities per direction for each section.

The control goal is to minimize the quadratic criterion

$$J_{LQI} = \frac{1}{2} \sum_{k_c=0}^{\infty} \left[ \|\mathbf{Ax}(k_c)\|_{\mathbf{Q}}^2 + \|\mathbf{y}(k_c)\|_{\mathbf{S}}^2 + \|\mathbf{u}(k_c)\|_{\mathbf{R}}^2 \right] \quad (19)$$

where  $\mathbf{Q} \in \mathbb{R}^{3n \times 3n}$ ,  $\mathbf{S} \in \mathbb{R}^{n \times n}$ ,  $\mathbf{R} \in \mathbb{R}^{n \times n}$  are symmetric positive definite matrices, which will be chosen in Section 4 to be diagonal for simplicity of tuning. The first term penalizes any deviation of the elements of the state variable

$\Delta \mathbf{x}$  from zero, i.e. any deviation of  $\tilde{\rho}_i^a(k)$ ,  $\tilde{\rho}_i^b(k)$ ,  $\gamma_i(k)$ ,  $i=1,2,\dots,n$  from their desired steady state values. The second term penalizes any deviation of the elements of the state variable  $\mathbf{y}$  from zero, i.e. any deviation of the integral of the differences between the relative densities per direction for each section from zero. Finally, the third term penalizes any deviation of the control input from the nominal values.

Considering the discrete-time linear system (17), (18) and the quadratic criterion (19), the following augmented problem matrices are defined

$$\tilde{\mathbf{A}} = \begin{bmatrix} \mathbf{A}^M & \mathbf{0} \\ \mathbf{H} & \mathbf{I} \end{bmatrix}, \tilde{\mathbf{B}} = \begin{bmatrix} \hat{\mathbf{B}} \\ \mathbf{0} \end{bmatrix}, \tilde{\mathbf{Q}} = \begin{bmatrix} \mathbf{Q} & \mathbf{0} \\ \mathbf{0} & \mathbf{S} \end{bmatrix}, \tilde{\mathbf{R}} = \mathbf{R} \quad (20)$$

#### D. Calculation of the LQI Regulator

Given the above specifications, the optimal controller minimizing the criterion is given by

$$\Delta \mathbf{u}(k_c) = -\mathbf{K} \begin{bmatrix} \Delta \mathbf{x}(k_c) \\ \mathbf{y}(k_c) \end{bmatrix} \quad (21)$$

where  $\mathbf{K} \in \mathbb{R}^{n \times 3n}$  is the constant gain matrix that can be calculated by iterating backwards in time (starting from any terminal positive semidefinite condition) the dynamic Riccati equation of the finite-horizon case until  $\mathbf{K}$  converges to a stationary value.

Decomposing the gain matrix  $\mathbf{K} = [\mathbf{K}_1, \mathbf{K}_2]$  and setting the nominal value of relative densities equal to 1, then, after some algebra, the final form of the Linear-Quadratic regulator with Integral action (LQI regulator) for the internal boundary control problem is given by

$$\begin{aligned} \boldsymbol{\varepsilon}(k_c) &= \boldsymbol{\varepsilon}(k_c - 1) - \\ &\mathbf{K}_p [\mathbf{x}(k_c) - \mathbf{x}(k_c - 1)] - \mathbf{K}_I [\tilde{\mathbf{p}}^a(k_c) - \tilde{\mathbf{p}}^b(k_c)] \end{aligned} \quad (22)$$

where  $\mathbf{K}_p = \mathbf{K}_1 - \mathbf{K}_2 \mathbf{H}$  and  $\mathbf{K}_I = \mathbf{K}_2$  are the proportional and integral gain matrices, respectively, while  $\boldsymbol{\varepsilon}(k_c) = [\varepsilon_1(k_c), \dots, \varepsilon_n(k_c)]^T$ ,  $\mathbf{x}(k_c) = [\tilde{\mathbf{p}}^a(k_c)^T, \tilde{\mathbf{p}}^b(k_c)^T, \boldsymbol{\gamma}(k_c)^T]^T$ ,  $\tilde{\mathbf{p}}^a(k_c) = [\tilde{\rho}_1^a(k_c), \dots, \tilde{\rho}_n^a(k_c)]^T$ ,  $\tilde{\mathbf{p}}^b(k_c) = [\tilde{\rho}_1^b(k_c), \dots, \tilde{\rho}_n^b(k_c)]^T$  and  $\boldsymbol{\gamma}(k_c) = [\gamma_1(k_c), \dots, \gamma_n(k_c)]^T$ .

The values obtained for each one of the control variables must be truncated before application in order to satisfy (3). These truncated values are used as  $\boldsymbol{\varepsilon}(k_c - 1)$  in (22) in the next time-step to avoid the well-known wind-up effect of regulators with integral terms.

## IV. SIMULATION INVESTIGATIONS

### A. Simulation Set-up

The performance of the proposed feedback-based controller is investigated using the bi-directional highway stretch depicted in Fig. 3. The considered highway stretch has

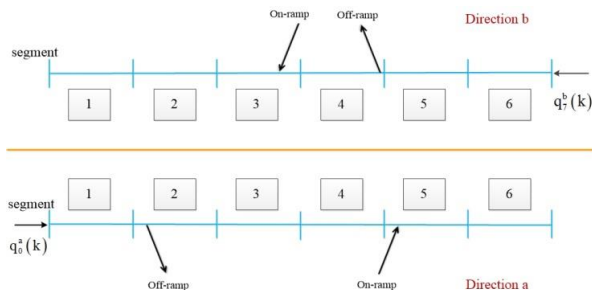


Fig. 3. The considered highway stretch.

a length of 3 km and is subdivided in 6 sections of 0.5 km each. The modelling time-step,  $T$ , is set to 10 s and the considered time horizon is 1 h. While a linearization of CTM was used for controller design, the full nonlinear CTM is used to represent the emulated ground truth in this section. The model parameters used are  $v_f = 100$  km/h and  $w_s = 12$  km/h; while the total cross-road capacity to be shared among the two directions is  $q_{cap} = 12,000$  veh/h. The exit rates for the two off-ramps are both set equal to 0.1.

The mainstream and on-ramp demand flows per direction are presented in Fig. 4. It may be seen that the two directions feature respective peaks in their mainstream demands that are slightly overlapping. In addition, the on-ramp demands are constant, with the on-ramp demand in direction  $a$  being higher than in direction  $b$ . The simulation results of the no-control case are presented first followed by the results obtained when using the LQI regulator.

### B. Regulator Design

In order to apply the feedback-based LQI regulator (22) developed in Section 3, we need to calculate off-line the static gain matrix  $\mathbf{K} = [\mathbf{K}_1, \mathbf{K}_2]$ . The convex combination parameter is selected to be  $\sigma = 0.95$ . A nominal point of operation is selected for the calculation of the matrices  $\mathbf{A}$  and  $\mathbf{B}$  used in the linear model (16). The nominal values are  $q_0^a|_N = q_7^b|_N = 5000$  veh/h,  $r_5^a|_N = r_3^b|_N = 1000$  veh/h,  $\rho_i^a|_N = \rho_i^b|_N = 1$  and  $\varepsilon_i|_N = 0.5$ ,  $i = 1, 2, \dots, 6$ . From (11), we can conclude that  $\gamma_i|_N = 0.5$ ,  $i = 1, 2, \dots, 6$ . The control time-step,  $T_c$ , is set to 60 s, hence  $M = 6$ . Based on (20) and the  $\mathbf{A}$  and  $\mathbf{B}$  matrices, we can calculate the  $\tilde{\mathbf{A}}$  and  $\tilde{\mathbf{B}}$  matrices for the augmented linear system. The weighing matrices used in the objective function (19) are selected to be  $\mathbf{Q} = [\mathbf{I}_{2n \times 2n}, \mathbf{0}_{n \times n}, \mathbf{0}_{n \times 3n}]$ ,  $\mathbf{S} = 10^{-2.5} \mathbf{I}_{n \times n}$  and  $\mathbf{R} = 10^{-3} \mathbf{I}_{n \times n}$ ; but good results are obtained for a range (around 1 decade) of values around these settings. This allows for the calculation of  $\tilde{\mathbf{Q}}$  and  $\tilde{\mathbf{R}}$ , and consequently of the gain matrix  $\mathbf{K}$ . The LQI regulator, employing the obtained gain matrix, is quite robust with respect to variations in the values of the selected weighing matrices. The corresponding analysis is not included here due to space limitations.

The LQI regulator (22) starts with initial control input values set equal to the nominal values, i.e. equal to 0.5 for all sections. The upper and lower bounds for the sharing factors, used to avoid utter blocking of any of the two directions, are equal for all sections  $i = 1, 2, \dots, 6$  and are given the values  $\varepsilon_{i,\min} = 0.16$  and  $\varepsilon_{i,\max} = 0.84$ .

With these settings, the regulator is operated in a closed loop mode, receiving in emulated real time all section density values per direction from the CTM model equations; and responding with the sharing factors calculated according to (22). This is repeated every  $T_c = 60$  s.

### C. No-control Case

Using the demand flows presented in Fig. 4 in the nonlinear CTM equations with constant sharing factor at  $\varepsilon_i = 0.5$  for all sections due to no internal boundary control, we obtain the simulation results of the no-control case with a TTS value equal to 209.8 veh·h. Fig. 5 displays the corresponding spatio-temporal evolution of the relative density defined in (9). According to the definition, relative density values lower than 1 refer to uncongested traffic; while values higher than 1 refer to congested traffic; when

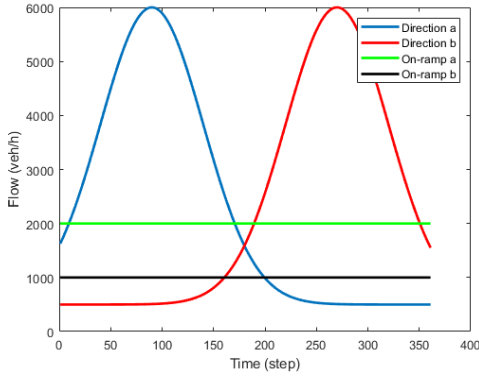


Fig. 4. Demand flows per direction and on-ramp.

the relative density equals 1, and the downstream section is uncongested, we have capacity flow at the corresponding section.

Fig. 5 shows that heavy congestion is created in section 5 for direction  $a$  due to the strong ramp inflow, in combination with the increased mainstream demand, at around  $k = 60$ . The congestion propagates upstream, reaching up to section 2, and dissolves at around  $k = 200$ , due to the rapid decrease of the mainstream demand for this direction. In direction  $b$ , we have also a congestion being triggered in section 4 by the increasing mainstream demand, in combination with the on-ramp flow, at around  $k = 260$ . Due to lower on-ramp flow, the congestion extent is smaller than in direction  $a$  and dissolves at around  $k = 330$ .

#### D. Control Case

Using the LQI regulator for the sharing factors, the resulting traffic conditions are under-critical everywhere as shown in the spatio-temporal evolution of the relative densities depicted in Fig. 6. More detailed information for this case is presented in Figs. 7-9. Each figure has two columns with the results of two respective sections; for each section (column), we provide three diagrams (rows):

- The first diagram shows the two traffic densities (in veh/km), for directions  $a$  and  $b$ , and the corresponding critical densities, which are changing according to the sharing factor in the section.
- The second diagram shows the two traffic flows, for directions  $a$  and  $b$ , and the corresponding capacities, which are changing according to the sharing factor in the section. In addition, the sum of both flows is also displayed (cyan curve).
- The third diagram shows the value of the control input, i.e. the sharing factor applied, as well as the constant bounds (black curves), which may lead to possible truncation of the control input.

The displayed results confirm that densities (flows) are always lower than the respective critical densities (capacities) in all sections and in both directions; hence traffic conditions are always and everywhere under-critical. In fact, the total-flow curve (for both directions) does not reach the total road capacity (of 12,000 veh/h) at any time anywhere. In short, congestion is utterly avoided and any occurring delays in the no-control case do not exist anymore.

The sharing factor trajectories of the sections reveal that this excellent outcome is enabled via a smooth swapping of assigned capacity to the two directions, whereby more

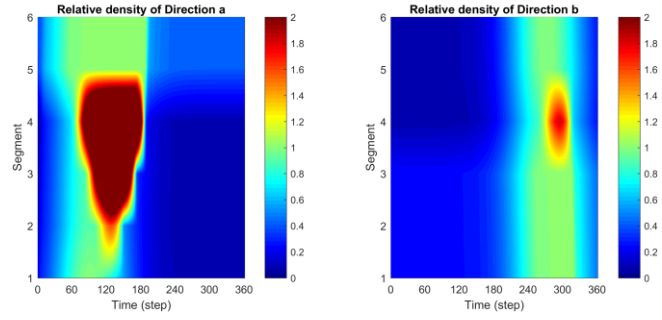


Fig. 5. Relative density for the two directions in the no-control case.

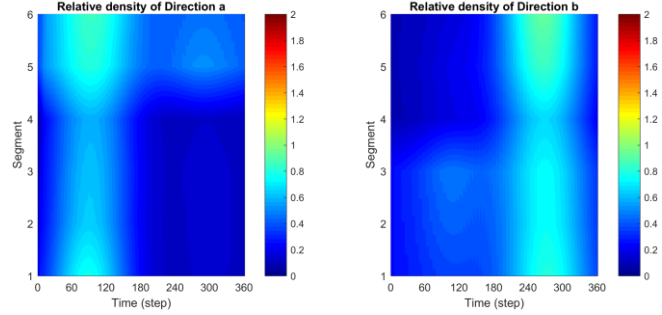


Fig. 6. Relative density for the two directions in the control case.

capacity is assigned to direction  $a$  during the first half of the time horizon and vice-versa for the second half, in response to the traffic (density) changes caused by the changing respective demands and their peaks. It is interesting to notice that the value of the control input (sharing factor) is never saturated.

The related TTS value is 164.9 veh·h, indicating an improvement of 21.4% over the no-control case. The TTS value obtained using the LQI regulator is, in fact, equal to the value that is achieved when applying the optimal control resulting from the QP problem formulation presented in [5]. Thus, despite its simple feedback character, where no demand predictions are used, the LQI regulator achieves highest efficiency for this scenario.

## V. CONCLUSIONS

The concept of internal boundary control, introduced in [5], has been revisited in this study by use of a different control algorithm. The well-known CTM, appropriately adjusted to introduce the effect of the sharing factors, has been utilized for the development of an LQI regulator for the internal boundary control problem. The total road width and capacity are shared in each section in real-time among the two directions of the road in response to the prevailing traffic conditions. The LQI regulator is easy to design and implement (feedback-based) and robust to disturbances (no need to predict the arriving demands). Simulation investigations demonstrate that the LQI regulator is equally efficient as an open-loop optimal control solution (with perfect model knowledge and demand prediction) developed for the same problem in [5] using a convex QP problem formulation.

Ongoing work considers microscopic simulation studies with vehicles moving in a lane-free mode, based on

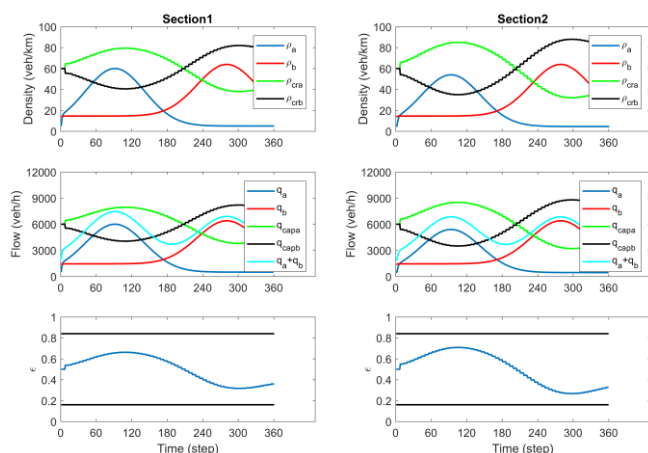


Fig. 7. Density, flow and control trajectories in the control case (sections 1 and 2).

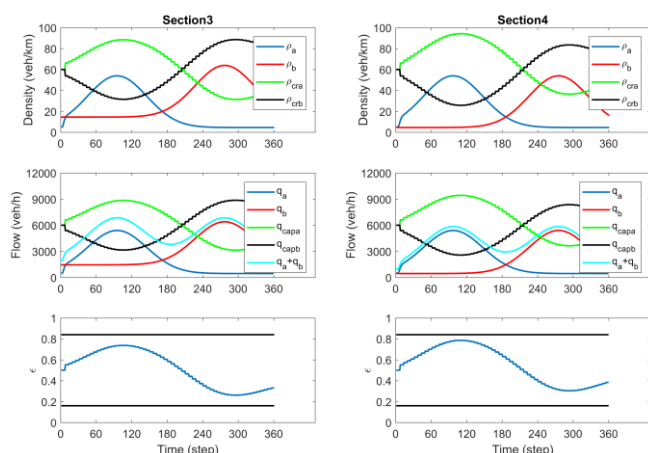


Fig. 8. Density, flow and control trajectories in the control case (sections 3 and 4).

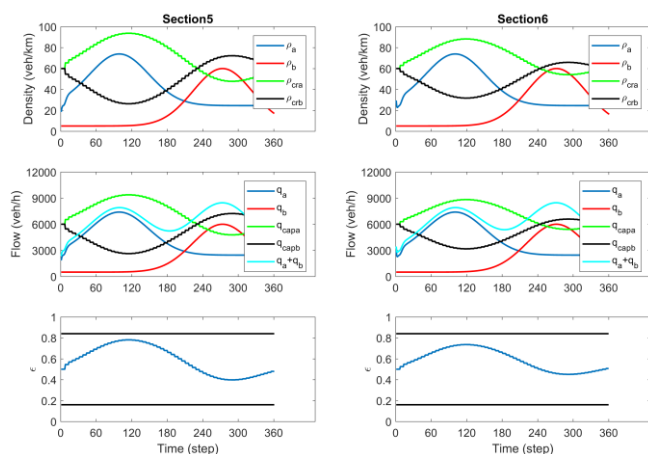


Fig. 9. Density, flow and control trajectories in the control case (sections 5 and 6).

appropriate CAV movement strategies. We also consider more realistic large-scale highway infrastructure scenarios.

## REFERENCES

- [1] M. Papageorgiou, C. Diakaki, V. Dinopoulou, A. Kotsialos, and Y. Wang, "Review of road traffic control strategies," *Proceedings of the IEEE*, vol. 91, no. 12, pp. 2043–2067, 2003.
- [2] A. A. Kurzhanskiy, and P. Varaiya, "Active traffic management on road networks: a macroscopic approach," *Philosophical Transactions of the Royal Society A: Mathematical, Physical and Engineering Sciences*, vol. 368, no. 1928, pp. 4607–4626, 2010.
- [3] C. Diakaki, M. Papageorgiou, I. Papamichail, and I. Nikolas, "Overview and analysis of vehicle automation and communication systems from a motorway traffic management perspective," *Transportation Research Part A: Policy and Practice*, vol. 75, pp. 147–165, 2015.
- [4] M. Papageorgiou, K. S. Mountakis, I. Karafyllis, I. Papamichail, and Y. Wang, "Lane-free artificial-fluid concept for vehicular traffic," *Proceeding of the IEEE*, vol. 109, pp. 114–121, 2021.
- [5] M. Malekzadeh, I. Papamichail, M. Papageorgiou, and K. Bogenberger, "Optimal internal boundary control of lane-free automated vehicle traffic," *Transportation Research Part C*, vol. 126, 103060, 2021.
- [6] B. Wolshon, and L. Lambert, "Reversible lane systems: Synthesis of practice," *Journal of Transportation Engineering*, vol. 132, no. 12, pp. 933–944, 2006.
- [7] J. R. D. Frejo, I. Papamichail, M. Papageorgiou, and E. F. Camacho, "Macroscopic modeling and control of reversible lanes on freeways," *IEEE Transactions on Intelligent Transportation Systems*, vol. 17, no. 4, pp. 948–959, 2015.
- [8] K. Ampountolas, J. A. dos Santos, and R. C. Carlson, "Motorway tidal flow lane control," *IEEE Transactions on Intelligent Transportation Systems*, vol. 21, no. 4, pp. 1687–1696, 2020.
- [9] A. K. Ziliaskopoulos, "A linear programming model for the single destination system optimum dynamic traffic assignment problem," *Transportation Science*, vol. 34, no. 1, pp. 37–49, 2000.
- [10] Y. Li, S. T. Waller, and A. K. Ziliaskopoulos, "A decomposition scheme for system optimal dynamic traffic assignment models," *Networks and Spatial Economics*, vol. 3, no. 4, pp. 441–455, 2003.
- [11] C. F. Daganzo, "The cell transmission model: A dynamic representation of highway traffic consistent with the hydrodynamic theory," *Transportation Research Part B: Methodological*, vol. 28, no. 4, pp. 269–287, 1994.
- [12] M. Duell, M. W. Levin, S. D. Boyles, and S. T. Waller, "System optimal dynamic lane reversal for autonomous vehicles," in *2015 IEEE 18th International Conference on Intelligent Transportation Systems*, pp. 1825–1830.
- [13] M. W. Levin, and S. D. Boyles, "A cell transmission model for dynamic lane reversal with autonomous vehicles," *Transportation Research Part C: Emerging Technologies*, vol. 68, pp. 126–143, 2016.
- [14] B. Bhavathrathan, and C. Mallikarjuna, "Evolution of macroscopic models for modeling the heterogeneous traffic: an Indian perspective," *Transportation Letters*, vol. 4, no. 1, pp. 29–39, 2012.
- [15] G. Asaithambi, V. Kanagaraj, and T. Toledo, "Driving behaviors: Models and challenges for non-lane based mixed traffic," *Transportation in Developing Economies*, vol. 2, no 19, 2016.
- [16] C. R. Munigety, and T. V. Mathew, "Towards behavioral modeling of drivers in mixed traffic conditions," *Transportation in Developing Economies*, vol. 2, no 6, 2016.
- [17] L. Isaksen, and H. J. Payne, "Suboptimal control of linear systems by augmentation with application to freeway traffic regulation," *IEEE Transactions on Automatic Control*, vol. 18, pp. 210–219, 1973.
- [18] M. Papageorgiou, "Multilayer control system design applied to freeway traffic," *IEEE Transactions on Automatic Control*, vol. 29, no. 6, pp. 482–490, 1984.
- [19] M. Papageorgiou, J.-M. Blosseville, and H. Hadj-Salem, "Modelling and real-time control of traffic flow on the southern part of Boulevard Périphérique in Paris - Part II: Coordinated on-ramp metering," *Transportation Research Part A: Policy and Practice*, vol. 24, no. 5, pp. 361–370, 1990.